Structural controlled magnetic anisotropy in Heusler $L1_0$–MnGa epitaxial thin films

Kangkang Wang,[1] Erdong Lu,[1,a)] Jacob W. Knepper,[2] Fengyuan Yang,[2] and Arthur R. Smith[1,b)]
[1]*Department of Physics and Astronomy, Nanoscale and Quantum Phenomena Institute, Ohio University, Athens, Ohio 45701, USA*
[2]*Department of Physics, Ohio State University, 191 Woodruff Ave., Columbus, Ohio 43210, USA*

(Received 16 February 2011; accepted 4 April 2011; published online 20 April 2011)

Ferromagnetic $L1_0$–MnGa thin films have been epitaxially grown on GaN, sapphire, and MgO substrates using molecular beam epitaxy. Using diffraction techniques, the epitaxial relationships are determined. It is found that the crystalline orientation of the films differ due to the influence of the substrate. By comparing the magnetic anisotropy to the structural properties, a clear correlation could be established indicating that the *in-plane* and *out-of-plane* anisotropy is directly determined by the crystal orientation of the film and could be controlled via selection of the substrates. This result could be helpful in tailoring magnetic anisotropy in thin films for spintronic applications. © *2011 American Institute of Physics*. [doi:10.1063/1.3582244]

Magnetic thin film on insulator and/or semiconductor hybrid systems are key components in important spintronic applications such as magnetic tunnel junctions (MTJs), gigabit nonvolatile memories, and spin injectors.[1,2] Observations of nonuniform behaviors and premature switching in nanometer-size MTJs have triggered remarkable interest in the search for crystalline thin films with canted or perpendicular magnetization, which allow the realization of highly reliable devices.[3,4] It is therefore crucial to explore reliable methods to control the magnetic anisotropy in crystalline thin films.

Here we report a crystal structural control of the magnetic anisotropy in thin epitaxial MnGa films. This Heusler alloy has drawn lots of attention recently for its many desirable properties such as high spin polarization and low damping term.[5–8] Furthermore, its magnetic properties depend sensitively on the Mn:Ga stoichiometry, ranging from ferromagnetic for MnGa,[2] to ferrimagnetic for $Mn_{2-3}Ga$,[5–8] and antiferromagnetic for Mn_3Ga,[9] giving this material great magnetic tunability. In this letter, we explore the epitaxial growth of $L1_0$-structured ferromagnetic MnGa thin films on various substrates including GaN, sapphire, and MgO. These thin films are found to exhibit different crystal orientations, which are shown to have direct impact on the magnetic anisotropy. This result provides an effective way for tuning the film magnetic anisotropy via controlling the crystalline properties.

Samples are grown in a custom-designed ultrahigh-vacuum molecular beam epitaxy chamber equipped with Mn and Ga effusion cells. Commercially available GaN(0001)/sapphire, sapphire(0001), and MgO(001) substrates are used in this study. All substrates are solvent cleaned *ex situ* and annealed *in situ* for 30 min (950 °C for sapphire and MgO, and 650 °C for GaN). For GaN substrate, a fresh 50-nm-thick layer of GaN is grown on top for improved surface smoothness. For the growth of up to 200-nm-thick MnGa layer, substrate temperatures are carefully maintained at 250 ± 30 °C and Mn:Ga flux ratios are maintained at ~55:45 (calibrated using a quartz flux sensor). All growths are monitored in real-time using reflection high-energy electron diffraction (RHEED). After growth, samples are transferred *ex situ* for x-ray diffraction (XRD) as well as vibrating sample magnetometery (VSM) measurements.

Figure 1 shows RHEED images before and after the growth of MnGa films on three different substrates. For MnGa/GaN [see Figs. 1(a) and 1(b)], the growth evolution is in agreement with the one reported before,[2] resulting in a nearly ideal epitaxial relationship with a 30° rotation between the two sublattices. The interface is found to be atomically abrupt, recently attributed to a two-dimensional Mn–Ga layer.[10] Figure 1(c) shows the surface of sapphire(0001) substrates along $[1\bar{1}00]$ prior to MnGa deposition; Kikuchi lines emerging from inelastic scattering are clearly visible at this stage. After the growth of MnGa, the primary streak spacing increases, together with the emergence of weak $2\times$ fractional streaks, indicating the existence of a surface superstructure [Fig. 1(d)]. We propose that the same 2×2 supercell induced by excess Mn atoms, as previously proposed for

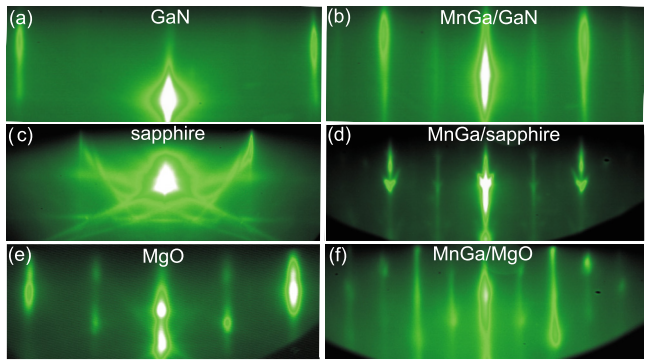

FIG. 1. (Color online) RHEED images during epitaxial growth of $L1_0$–MnGa on different substrates. Left column: annealed substrate surfaces; right column: after growth of MnGa. (a) and (b) Along $[1\bar{1}00]_{GaN}$. (c) and (d) Along $[1\bar{1}00]_{sapphire}$. (e) and (f) Along $[110]_{MgO}$.

a)Present address: Richter Precision Inc., 1021 Commercial Ave., East Petersburg, Pennsylvania 17520, USA.
b)Electronic mail: smitha2@ohio.edu.

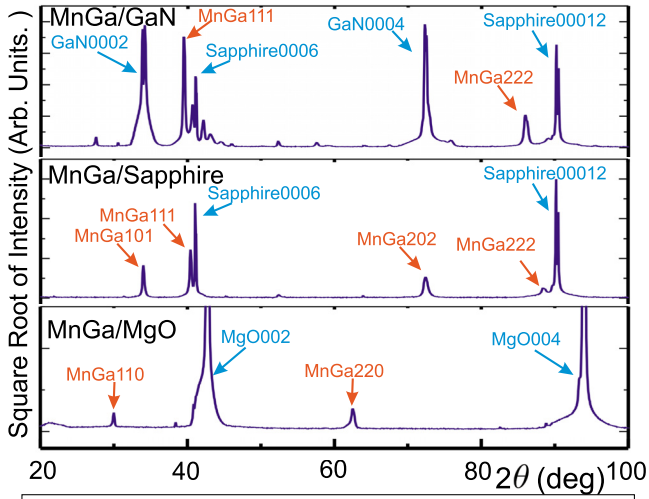

	MnGa/GaN	MnGa/Sapphire	MnGa/MgO
a (Å)	3.91	3.98	4.11
c (Å)	3.77	3.52	3.67

FIG. 2. (Color online) θ-2θ XRD spectra of the epitaxial $L1_0$−MnGa films grown on various substrates at 250 °C. Main peaks are identified and marked in each figure; lower panel: table summarizing derived lattice constants.

MnGa/GaN,[2] could also be responsible for the 2× observed here. Furthermore, chevron (arrow-head shaped) features are observed along the primary streaks, suggesting multiple facets at the surface, which can be linked to the coexistence of multiple structural domains.[11] For the growth on MgO(001) [Figs. 1(e) and 1(f)], 2× fractional streaks are also observed, but without chevron features. For all the MnGa films grown, the observed RHEED patterns remain bright and streaky, absent of rings (polycrystalline) or highly diffusive backgrounds (amorphous). This indicates that the films are highly crystalline and have atomically smooth surfaces. It is noted that maintaining a substrate temperature at around 250 °C is crucial in obtaining this high crystallinity.

To further determine the crystal structure of the MnGa thin films, we performed XRD with a Cu $K\alpha$ source on the epitaxial films. As shown in Fig. 2, all the films are determined to have the $L1_0$ face-centered tetragonal structure as previously reported by Niida *et al.*[12] By comparing the lattice spacings derived from the observed XRD peaks with the calculated d spacings based on the known bulk CuAu-$L1_0$ structure (a=3.89 Å and c=3.65 Å), the film orientations could be determined to be (111) for MnGa/GaN(0001), coexisting (111) and (101) for MnGa/sapphire(0001), and (110) for MnGa/MgO(001). Lattice constants for our films are derived and summarized in the lower panel of Fig. 2.

The epitaxial relationships can then be determined by computing the *in-plane* lattice spacings based on the primary streak spacings in the RHEED patterns, and comparing to possible in-plane relations. For MnGa(111)/GaN(0001), the same epitaxial relationship as previously reported is derived, namely, $[1\bar{1}0]_{\mathrm{MnGa}}\|[1\bar{1}00]_{\mathrm{GaN}}$ and $[11\bar{2}]_{\mathrm{MnGa}}\|[11\bar{2}0]_{\mathrm{GaN}}$. For MnGa(111)/sapphire(0001), the epitaxial relationship is determined to be $[1\bar{1}0]_{\mathrm{MnGa}}\|[1\bar{1}00]_{\mathrm{sapphire}}$ and $[11\bar{2}]_{\mathrm{MnGa}}\|[11\bar{2}0]_{\mathrm{sapphire}}$. The in-plane orientation for the other coexisting (101) domain could not be easily determined because the RHEED pattern is dominated by the (111) domain. For MnGa(110)/MgO(001), we obtain $[1\bar{1}0]_{\mathrm{MnGa}}\|[1\bar{1}0]_{\mathrm{MgO}}$ and $[001]_{\mathrm{MnGa}}\|[110]_{\mathrm{MgO}}$.

Note that while both GaN and sapphire are hexagonal structured, we find coexistence of two different crystalline domains [(111) and (101)] for the MnGa film grown on sapphire(0001). This could be due to a larger lattice mismatch compared to the growth on GaN(0001). By integrating the area under the main peaks (A_{111} and A_{101}), and normalizing them using structure factors F_{hkl},[13] the ratio R of atomic concentrations of the two differently oriented crystallites can be estimated by $R=A_{111}/|F_{111}|^2/(A_{101}/|F_{101}|^2)$. We find that ~61% of the film is (111) oriented while the rest (~39%) is (101) oriented.

To explore how these structural differences affect the magnetism, VSM measurements are carried out at room temperature on these $L1_0$−MnGa thin films with both in-plane and *out-of-plane* magnetic configurations. The magnetic hysteresis loops are displayed in Figs. 3(a)–3(c), where the magnetization values are normalized by the sample volume. Magnetic parameters are summarized in the table shown in Fig. 3(d).

It is interesting to compare the magnetic anisotropy to the crystalline structure of the film. In bulk materials, the *magnetocrystalline* anisotropy often plays the dominant role in the overall magnetic anisotropy. It is therefore natural to consider this crystalline anisotropy as the main source here as well for the anisotropy observed in our $L1_0$−MnGa thin films. Assuming an easy axis anisotropy, based on the Stoner–Wohlfarth coherent rotation model,[14] the total energy density consists of an anisotropy term and a Zeeman energy

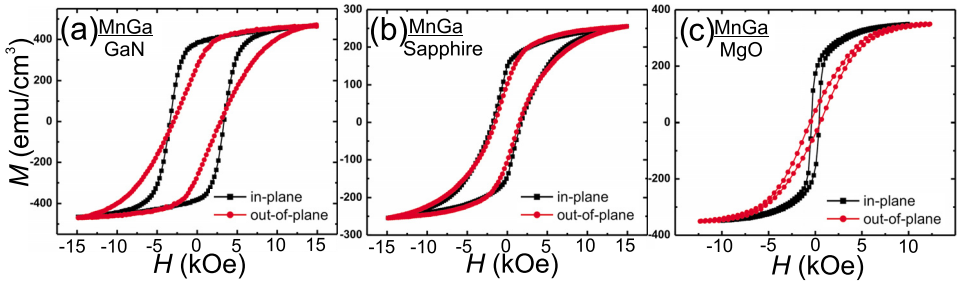

(d)	M_s	$M_{r\|\|}$	$M_{r\perp}$	$H_{c\|\|}$	$H_{c\perp}$	Θ
MnGa/GaN	464	384	273	3.35	2.97	54.6
MnGa/Sapphire	255	141	113	1.72	1.47	51.3
MnGa/MgO	349	171	23	0.41	0.49	82.3

FIG. 3. (Color online) [(a)–(c)] In-plane and out-of-plane magnetic hysteresis loops of the $L1_0$−MnGa films grown on various substrates. (d) Table summarizing the saturation magnetization M_s; in-plane and out-of-plane remnant magnetization $M_{r\|}$ and $M_{r\perp}$ (emu/cm^3); coercive fields $H_{c\|}$ and $H_{c\perp}$ (kOe); and calculated easy axis angle Θ (deg) with respect to the film normal for the grown films.

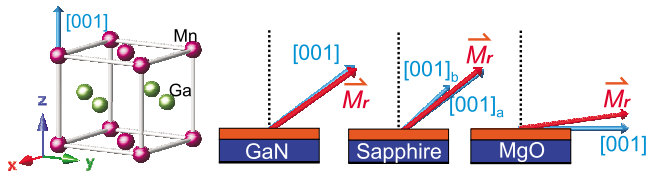

FIG. 4. (Color online) Left: Unit cell of $L1_0$−MnGa. Right: Comparison of the [001] crystalline directions with the determined magnetic easy axis ($\vec{M}_r$). For MnGa/sapphire, $[001]_a$ corresponds to the (111) oriented domain and $[001]_b$ corresponds to (101) oriented domain, with length weighted based on atomic concentration.

term; $E/V=K\sin^2(\phi-\theta)-\mu_0 M_s H\cos\phi$, where ϕ is the angle between the sample magnetization and the external field direction, θ is the angle between the easy axis and the external field direction, and K is the anisotropy constant. The hysteresis loop is obtained by solving the stability equations $\partial E/\partial\phi=0$ and $\partial^2 E/\partial\phi^2>0$. The remnant magnetization along the field direction can then be derived to be $M_r=M_s\cos\theta$. Therefore one could use the measured in-plane and out-of-plane remnant magnetization values to calculate the easy axis direction of the film: $\Theta=\tan^{-1}(M_{r\parallel}/M_{r\perp})$, where Θ is the angle between the easy axis and the film surface normal.

The Θ values for the various $L1_0$−MnGa films are computed and directly compared to the angle of the [001] crystalline direction with respect to the film normal ($\theta_{[001]}$) determined for the corresponding films, as shown in Fig. 4. In all cases, we find that Θ is close to $\theta_{[001]}$. For MnGa/sapphire, there are two different [001] directions corresponding to the two structural domains [(111) and (101)]; in this case, Θ is slightly closer to $\theta_{[001]}$ of the dominant crystalline domain (see Fig. 4 caption). This trend is also consistent with previous reports of perpendicular magnetization observed for MnGa films grown along the [001] direction on GaAs.[15] We note that, compared to MnGa/GaN and MnGa/sapphire, the slightly larger difference between Θ and $\theta_{[001]}$ observed for the MnGa/MgO films could be an inherent drawback originating from the oversimplification in the Stoner–Wohlfarth model. This model predicts zero remnant magnetization along perpendicular-to-easy-axis directions, which is rarely observed due of incoherency in the sample magnetic moments such as pinned domains.

The close relation between the easy magnetization axis and the crystalline orientation indicates that the same easy axis magnetic anisotropy remains dominant for films grown on different substrates, given that the films are highly crystalline and not too much distorted from the bulk lattice. The direct impact of the film orientation on the magnetic anisotropy provides a method for controlling the anisotropy direction in thin crystalline films. Here, this control is realized by selecting different substrates; however, other routes such as using a buffer layer during growth, or varying the Mn:Ga ratio, could also enable tailoring of the anisotropy. Recently, premature switching in MTJs have been attributed to defects in the junctions, whose microstructure has been studied by transmission electron microscopy showing local misorientations.[16] Our result here, namely, that film orientations could directly modify the magnetic anisotropy, can be one explanation for these nonuniform behaviors.

In conclusion, we have studied the epitaxial growth of Heusler $L1_0$−MnGa thin films on different substrates. The crystalline orientations as well as the in-plane epitaxial relationships are derived based on diffraction measurements. A direct link is found between the crystalline orientation and the resulting magnetic anisotropy, explained by a simple easy-axis magnetic anisotropy model. These results provide a reliable method for tailoring the magnetic anisotropy in crystalline thin films via controlling the crystalline structure, and could potentially lead to successful applications in a variety of spintronic devices.

This study is supported by the Department of Energy, Office of Basic Energy Sciences (Grant No. DE-FG02-06ER46317) and by the National Science Foundation (Grant No. 0730257).

[1] S. S. P. Parkin, C. Kaiser, A. Panchula, P. M. Rice, B. Hughes, M. Samant, and S. H. Yang, Nature Mater. **3**, 862 (2004).
[2] E. Lu, D. C. Ingram, A. R. Smith, J. W. Knepper, and F. Y. Yang, Phys. Rev. Lett. **97**, 146101 (2006).
[3] G. Kim, Y. Sakuraba, M. Oogane, Y. Ando, and T. Miyazaki, Appl. Phys. Lett. **92**, 172502 (2008).
[4] S. Ikeda, K. Miura, H. Yamamoto, K. Mizunuma, H. D. Gan, M. Endo, S. Kanai, J. Hayakawa, F. Matsukura, and H. Ohno, Nature Mater. **9**, 721 (2010).
[5] F. Wu, E. P. Sajitha, S. Mizukami, D. Watanabe, T. Miyazaki, H. Naganuma, M. Oogane, and Y. Ando, Appl. Phys. Lett. **96**, 042505 (2010).
[6] F. Wu, S. Mizukami, D. Watanabe, H. Naganuma, M. Oogane, Y. Ando, and T. Miyazaki, Appl. Phys. Lett. **94**, 122503 (2009).
[7] B. Balke, G. H. Fecher, J. Winterlik, and C. Felser, Appl. Phys. Lett. **90**, 152504 (2007).
[8] H. Kurt, K. Rode, M. Venkatesan, P. S. Stamenov, and J. M. D. Coey, Phys. Rev. B **83**, 020405 (2011).
[9] H. Niida, T. Hori, and Y. Nakagawa, J. Phys. Soc. Jpn. **52**, 1512 (1983).
[10] K. Wang, N. Takeuchi, A. V. Chinchore, W. Lin, Y. Liu, and A. R. Smith, Phys. Rev. B **83**, 165407 (2011).
[11] H. Lee, R. Lowe-Webb, W. Yang, and P. C. Sercel, Appl. Phys. Lett. **72**, 812 (1998).
[12] H. Niida, T. Hori, H. Onodera, Y. Yamaguchi, and Y. Nakagawa, J. Appl. Phys. **79**, 5946 (1996).
[13] Structure factors are computed using *Powdercell* (BAM federal institute for materials research and testing, Berlin).
[14] R. Skomski, *Simple models of magnetism* (Oxford University Press, Oxford, 2008), Chap. 4.
[15] K. M. Krishnan, Appl. Phys. Lett. **61**, 2365 (1992).
[16] J. W. Lau, P. Morrow, J. C. Read, V. Höink, W. F. Egelhoff, L. Huang, and Y. Zhu, Appl. Phys. Lett. **96**, 262508 (2010).